



## Review Article

Volume 4 Issue 3 - April 2018  
DOI: 10.19080/JOJMS.2018.04.555637

JOJ Material Sci

Copyright © All rights are reserved by Rajesh Kumar Singh

# Mild steel Corrosion Control by the Nanocoating and Filler Compounds in Hostile Environments

**Rajesh Kumar Singh<sup>1\*</sup>, Manjay Kumar Thakur<sup>2</sup> and Shabana Latif<sup>2</sup>**<sup>1</sup>Department of Chemistry, Jagdam College, J P University, Chpara-84130, India<sup>2</sup>Research Scholar, Department of Chemistry, Jagdam College, J P University, Chapra, India

Submitted: April 10, 2018; Published: April 23, 2018

**\*Corresponding author:** Rajesh Kumar Singh, Department of Chemistry, Jagdam College, JP University, Chpara-84130, India;  
Email: rks\_jpujc@yahoo.co.in

## Abstract

Mild steel is protected by polymeric coating of polybutadiene. But this coating is not shaved mild steel in moist air, sulphur dioxide and chloride environment. These pollutants interact with polybutadiene-coated mild steel and create hostile atmosphere their surroundings. Moist air accommodates on the surface of polymeric-coated metal which absorb sulphur dioxide to form sulphuric acid. It produces chemical and electrochemical reaction with polymeric-coated metal and accelerates corrosion reaction. Chloride ions are entered inside by osmosis or diffusion process and develop corrosion cell on metal surface. Oxygen deficiency occurs inside and outside of polymeric-coated mild steel thus corrosion cell automatically produced. These pollutants in this ways start interior and exterior corrosion of polymeric-coated metal. These pollutants rupture internal bond of polybutadiene and produce disbonding between base metal and coating material. Metal exhibits various form of corrosion like galvanic, pitting, stress, crevice, blistering, embrittlement etc. Nanocoating and filler technique used to mitigate corrosion of materials in such corrosive environment. Octahydrodibenzo[a,d][8]annulene-5,12-dihydrazone used a nanocoating material whereas MgS as filler. Corrosion rate of polymeric-coated mild steel was determined by gravimetric methods and corrosion potential, corrosion current and corrosion current density were calculated by potentiostat. Nozzle sprays used for nanocoating. The surface adsorption phenomenon studied with application Langmuir isotherm and Arrhenius equation. Surface deposition and bond formation of nanocoating and filler materials were understood by activation energy, heat of adsorption, free energy, enthalpy and entropy. The experimental results surface coverage area and coating efficiency were shown that the used nanocoating and filler materials were developed composite thin film barrier on surface of polybutadiene-coated mild steel.

**Keywords:** Polybutadiene-coated mild steel; nanocoating, filler; pollutants; composite thin film barrier

## Introduction

Corrosion protection of materials is very difficult task. It is not fully control but this effect is minimized by the application of corrosion mitigation techniques. It is necessary for materials manufacturing industries to monitor carefully their internal morphology, shape and design. Materials can be synthesized Bhadra S et al. [1] as per need of surrounding environment Szabo T [2] which does not change their physical, chemical and biological properties Wen NT et al. [3] and provide thermal stability, durability, capability, resistance power against corrosive medium Boerio FJ et al. [4]. Materials corrosion protection Deveci H [5] check with application of coatings, inhibitors, sacrificial anodic protection and impressed current process are in ambient environment Genzer J et al. [6]. There are various types of coating available like metallic, nonmetallic, polymeric and paint. Such coatings do not protect materials longer times. Inhibitors Leon Silva U et al. [7] are used to control corrosion of metal in petroleum industries. Inhibitors are utilized in several forms Baier RE [8] like organic, inorganic and mixed types

inhibitors which are related to anodic as well as cathodic. Their application Rao BVA et al. [9] can be done in the form Liu XY et al. [10] of solid, liquid and gas as requirement of corrosive medium. Electron rich compounds Liao QQ et al. [11] alkane, alkene, alkyne, cyclic, aromatic and heterocyclic contain nitrogen, oxygen and sulphur are used as organic inhibitors in petroleum industries Zhang DQ et al. [12], sugar industries Sahoo RR et al. [13], phosphate industries Raman R et al. [14], pulp and paper industries Li D G et al. [15] to control the corrosion of mild steel Cristiani P et al. [16] and stainless steel Cristiani P et al. [17]. These inhibitors do not provide protection longer periods Videla H et al. [18]. Metallic pipe corrosion Bibber JW et al. [19] is mitigated by anodic protection and impressed current but they do not give good results in aggressive medium Ghareba GS et al. [20]. Aloe Vera is used check corrosion metallic can Singh RK [21] which contain beverages, orange juice, milk and vegetables. It works as natural inhibitor. In acidic soil the life of earthworms Singh RK [22] become miserable such environment their life can

be protected by the application aloe vera juice. Human skin is face corrosion problem in mega and metro cities environment such corrosion is control by the use of aloe vera and turmeric coating. Nanocoating and filler compounds Singh RK [23] are used to control the corrosion of polymeric-coated metal in ambient of effluents.

## Experimental

Mild steel sample (5X10X0.1) cm<sup>2</sup> was coated with polybutadiene and kept in SO<sub>2</sub> moist and Cl<sup>-</sup> ions. The sample corrosion rate were determined by gravimetric technique at 283, 293, 303, 312 and 3230K temperatures and that temperatures expose times were 3, 5, 8, 11 and 14days. These samples were nanocoated with octahydrodibenzo[a,d][8]annulene-5,12-dihydrazone and corrosion rate calculated at above mentioned temperatures and days. Nanocoated samples were again coated with MgS and measured corrosion rates. Potentiostat technique

used to calculate corrosion potential, corrosion current, corrosion current densities of sample without and with nanocoating above mentioned materials. Potentiostat consists pt electrode used as reference electrode, calomel as auxiliary electrode and polybutadiene-coated mild steel sample electrode and this electrode can be with octahydrodibenzo[a,d][8]annulene-5,12-dihydrazone and coating with MgS. Nanocoated compound octahydrodibenzo[a,d][8]annulene-5,12-dihydrazone was synthesized by given methods as.

### Scheme1: Synthesis of 4-Chloro-1, 2-Dihydronaphthalene:

When 3,4-dihydronaphthalen-1(2H)-one (25gm) is added into cold solution of benzene (50gm) containing PCl<sub>5</sub>(30gm), the reaction mixture was stirred for one hour. The reaction mixture was quenched with NaHCO<sub>3</sub> and did workup with diethyl ether. The solvent evaporated with rotator vapour. The product was purified by silica gel column chromatography and produced 89% 4-chloro-1, 2-dihydronaphthalene (Figure 1).

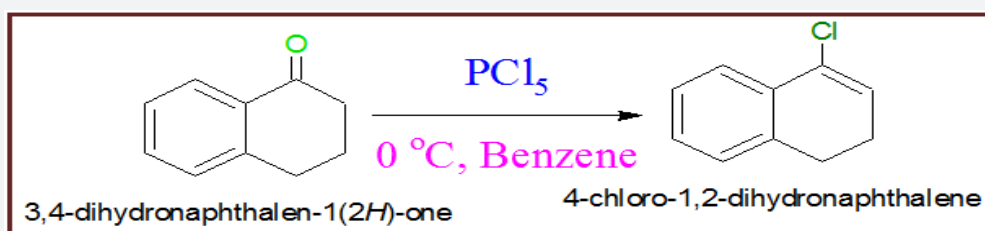


Figure 1.

	Molecular Formula	= C <sub>10</sub> H <sub>9</sub> Cl
	Formula Weight	= 164.63146
	Composition	= C(72.96%) H(5.51%) Cl(21.53%)
	Molar Refractivity	= 47.73 ± 0.4 cm <sup>3</sup>
	Molar Volume	= 141.2 ± 5.0 cm <sup>3</sup>
	Parachor	= 355.3 ± 6.0 cm <sup>3</sup>
	Index of Refraction	= 1.590 ± 0.03
	Surface Tension	= 40.0 ± 5.0 dyne/cm
	Density	= 1.16 ± 0.1 g/cm <sup>3</sup>
	Dielectric Constant	= Not available
	Polarizability	= 18.92 ± 0.5 10 <sup>-24</sup> cm <sup>3</sup>
	Monoisotopic Mass	= 164.039278 Da
	Nominal Mass	= 164 Da
	Average Mass	= 164.6315 Da

Figure 2.

### Physical properties of 4-chloro-1, 2-dihydronaphthalene

(Figure 2)

### <sup>1</sup>H NMR of 4-Chloro-1, 2-Dihydronaphthalene

(Figure 3)

### Scheme2: Synthesis of 1,2-Didehydro-3,4-Dihydronaphthalene:

4-Chloro-1,2-dihydronaphthalene (10gm) kept in two neck

round bottle flask and potassium t-butoxide (25gm) dissolved in THF solution. This solution poured into 4-Chloro-1,2-dihydronaphthalene and reaction temperature 00C. The reaction was mixture stirring four hours after completion reaction added cyclohexene as trapping agent and again stirring reaction more two hours. After work up got adduct 90% of 1,2-didehydro-3,4-dihydronaphthalene (Figure 4).

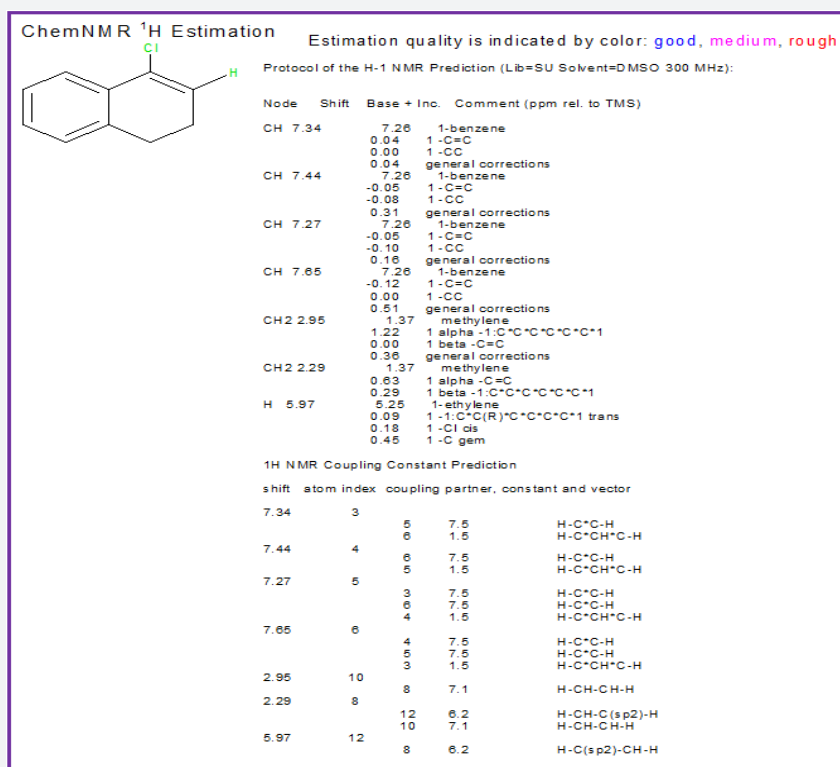


Figure 3.

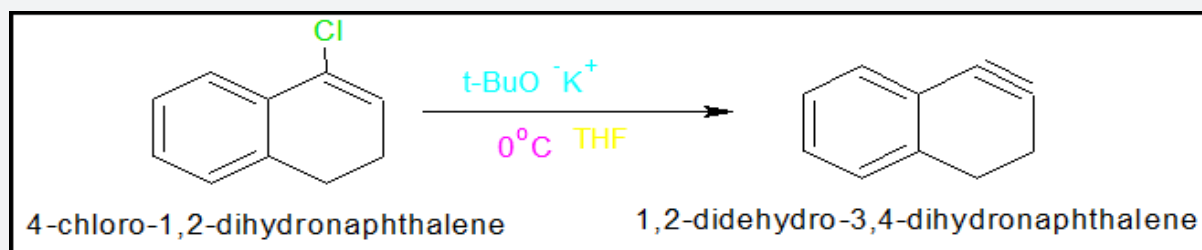


Figure 4.

### Physical Properties of 1,2-Didehydronaphthalene

(Figure 5)

	Molecular Formula	= C <sub>10</sub> H <sub>8</sub>
	Formula Weight	= 128.17052
	Composition	= C(93.71%) H(6.29%)
	Molar Refractivity	= 41.23 ± 0.4 cm <sup>3</sup>
	Molar Volume	= 119.7 ± 5.0 cm <sup>3</sup>
	Parachor	= 309.8 ± 6.0 cm <sup>3</sup>
	Index of Refraction	= 1.604 ± 0.03
	Surface Tension	= 44.8 ± 5.0 dyne/cm
	Density	= 1.07 ± 0.1 g/cm <sup>3</sup>
	Dielectric Constant	= Not available
	Polarizability	= 16.34 ± 0.5 10 <sup>-24</sup> cm <sup>3</sup>
	Monoisotopic Mass	= 128.0626 Da
	Nominal Mass	= 128 Da
	Average Mass	= 128.1705 Da
	M+	= 128.062052 Da
	M-	= 128.063149 Da
	[M+H] <sup>+</sup>	= 129.069877 Da
	[M+H] <sup>-</sup>	= 129.070974 Da
	[M-H] <sup>+</sup>	= 127.054227 Da
	[M-H] <sup>-</sup>	= 127.055324 Da

Figure 5.

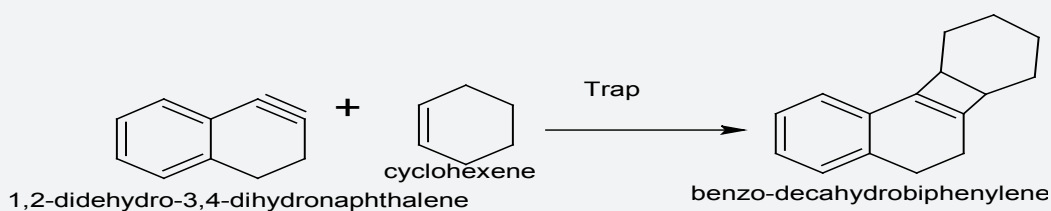
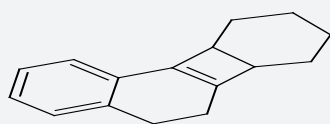


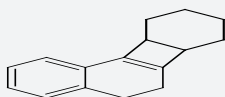
Figure 6.



Molecular Formula	= C <sub>18</sub> H <sub>18</sub>
Formula Weight	= 210.31412
Composition	= C(91.37%) H(8.63%)
Molar Refractivity	= 66.33 ± 0.4 cm <sup>3</sup>
Molar Volume	= 191.6 ± 5.0 cm <sup>3</sup>
Parachor	= 490.1 ± 6.0 cm <sup>3</sup>
Index of Refraction	= 1.608 ± 0.03
Surface Tension	= 42.7 ± 5.0 dyne/cm
Density	= 1.09 ± 0.1 g/cm <sup>3</sup>
Dielectric Constant	= 3.09 ± 0.2
Polarizability	= 26.29 ± 0.5 10 <sup>-24</sup> cm <sup>3</sup>
Monoisotopic Mass	= 210.140851 Da
Nominal Mass	= 210 Da
Average Mass	= 210.3141 Da
M+	= 210.140302 Da
[M+H] <sup>+</sup>	= 211.148127 Da
[M+H] <sup>-</sup>	= 211.149224 Da
[M-H] <sup>+</sup>	= 209.132477 Da
[M-H] <sup>-</sup>	= 209.133574 Da

Figure 7.

### ChemNMR <sup>1</sup>H Estimation



Estimation quality is indicated by color: **good**, **medium**, **rough**

Protocol of the <sup>1</sup>H-NMR Prediction (Lib=SU Solvent=DMSO 300 MHz):

Node Shift Base + Inc. Comment (ppm rel. to TMS)

CH 2.15	1.44	cyclohexene
	0.68	1 alpha-C=C from methine
	0.03	1 beta-C=C from methine
CH 2.15	1.44	cyclohexene
	0.68	1 alpha-C=C from methine
	0.03	1 beta-C=C from methine
CH2 2.34,2.240000	1.37	methylene
	0.63	1 alpha-C=C
	0.29	1 beta-1,2-C-C-C-C-C-C
CH2 1.41,1.310000	1.44	cyclohexene
	0.00	1 beta-C=C from methylene
	-0.08	generalconnections
CH2 1.41,1.310000	1.44	cyclohexene
	0.00	1 beta-C=C from methylene
	-0.08	generalconnections
CH 7.34	7.26	1-benzene
	0.04	1-C=C
	0.00	1-C-C
	0.04	generalconnections
CH 7.44	7.26	1-benzene
	-0.05	1-C=C
	-0.08	1-C-C
	0.31	generalconnections
CH 7.27	7.26	1-benzene
	-0.05	1-C=C
	-0.10	1-C-C
	0.16	generalconnections
CH 7.65	7.26	1-benzene
	-0.12	1-C=C
	0.00	1-C-C
	0.51	generalconnections
CH2 2.59	1.37	methylene
	1.22	1 alpha-1,2-C-C-C-C-C-C
	0.00	1 beta-C=C
CH2 1.53,1.430000	1.44	cyclohexene
	0.04	generalconnections
CH2 1.53,1.430000	1.44	cyclohexene
	0.04	generalconnections

<sup>1</sup>H NMR Coupling Constant Prediction

shift: atom index coupling partner, constant and vector

2.15	12	11	7.0	H-C-C-H
		16	7.0	H-C-C-H
2.15	11	12	7.0	H-C-C-H
		13	7.0	H-C-C-H
2.29	8	diastereotopic	-12.4	H-C-H
1.36	16	diastereotopic	-12.4	H-C-H
		10	7.1	H-C-H
		12	7.0	H-C-H
1.36	13	diastereotopic	-12.4	H-C-H
		11	7.0	H-C-H
		14	7.1	H-C-H
7.34	3	5	7.5	H-C-C-H
		6	1.5	H-C-C-H
7.44	4	6	7.5	H-C-C-H
		5	1.5	H-C-C-H
7.27	5	3	7.5	H-C-C-H
		6	7.5	H-C-C-H
		4	1.5	H-C-C-H
7.65	6	4	7.5	H-C-C-H
		5	7.5	H-C-C-H
		3	1.5	H-C-C-H
2.59	10	8	7.1	H-C-H
1.48	15	diastereotopic	-12.4	H-C-H
		16	7.1	H-C-H
		14	7.1	H-C-H
1.48	14	diastereotopic	-12.4	H-C-H
		13	7.1	H-C-H
		15	7.1	H-C-H

Figure 8.

### Scheme3: Synthesis of benzo-decahydrobiphenylene:

When 1,2-didehydro-3,4-dihydronaphthalene was used with cyclohexene, it was trapped by 1,2-didehydro-3,4-dihydronaphthalene to yield benzo-decahydrobiphenylene (Figure 6).

### Physical Properties of Benzo-Decahydrobiphenylene

(Figure 7)

### <sup>1</sup>H NMR of Benzo-Decahydrobiphenylene

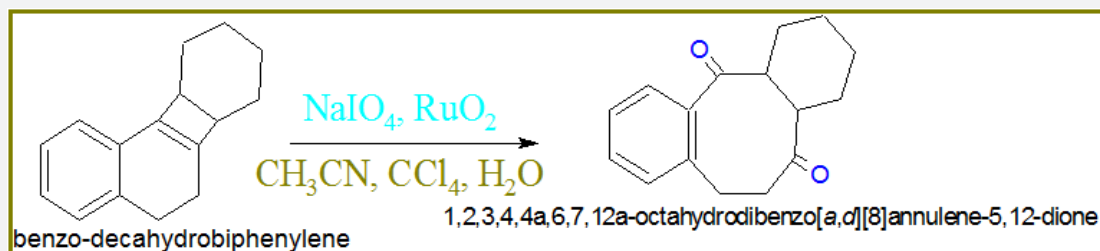
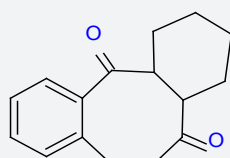


Figure 9.

### Physical Properties of Octahydrodibenzo[A,D][8]Annulene-5,12-Dione

(Figure 10)



Molecular Formula	= C <sub>16</sub> H <sub>18</sub> O <sub>2</sub>
Formula Weight	= 242.31292
Composition	= C(79.31%) H(7.49%) O(13.21%)
Molar Refractivity	= 69.02 ± 0.3 cm <sup>3</sup>
Molar Volume	= 216.7 ± 3.0 cm <sup>3</sup>
Parachor	= 549.8 ± 6.0 cm <sup>3</sup>
Index of Refraction	= 1.549 ± 0.02
Surface Tension	= 41.4 ± 3.0 dyne/cm
Density	= 1.118 ± 0.06 g/cm <sup>3</sup>
Dielectric Constant	= Not available
Polarizability	= 27.36 ± 0.5 10 <sup>-24</sup> cm <sup>3</sup>
Monoisotopic Mass	= 242.13068 Da
Nominal Mass	= 242 Da
Average Mass	= 242.3129 Da
M+	= 242.130131 Da
M-	= 242.131228 Da
[M+H] <sup>+</sup>	= 243.137956 Da
[M+H] <sup>-</sup>	= 243.139053 Da
[M-H] <sup>+</sup>	= 241.122306 Da
[M-H] <sup>-</sup>	= 241.123403 Da

Figure 10.

### <sup>1</sup>H NMR of octahydrodibenzo[a,d][8]annulene-5,12-dione

(Figure 11)

**Scheme5: Synthesis of Octahydrodibenzo[A,D][8]Annulene-5,12-Dihydrazone:** Octahydrodibenzo[a,d][8]annulene-5,12-dione (35g) was taken in a round bottomed flask and 75g of hydrazine hydrate was added and the mixture was heated under reflux for 24 hours. The solution was cooled in an ice bath and the octahydrodibenzo[a,d][8]annulene-5,12-dihydrazone was separated by suction filtration. The crystals were washed with 150ml of cold ethanol and dried on the suction filter for 1 hour. The yield of octahydrodibenzo[a,d][8]annulene-5,12-dioxime 90% was obtained (Figure 12).

### Physical properties of Octahydrodibenzo[A,D][8]Annulene-

(Figure 8)

**Scheme4: Synthesis of Octahydrodibenzo[A,D][8]Annulene-5,12-Dione:** Adduct (20gm) oxidized into benzo-decahydrobiphenylene with addition of NaIO<sub>4</sub> (10gm) and RuO<sub>2</sub> (15g) in the presence of solvent CH<sub>3</sub>CN and CCl<sub>4</sub>. The reaction was quenched with H<sub>2</sub>O and after workup 87% yield of octahydrodibenzo[a,d][8]annulene-5,12-dione was obtained (Figure 9).

### 5,12-Dihydrazone

(Figure 13 & 14)

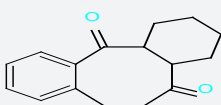
## Results and Discussion

Octahydrobenzo[a,d][8]annulene-5,12-dihydrazone was nanocoated on the surface of polybutadiene-coated mild steel and their porosities were blocked by MgS filler. The corrosion of metal was determined in marine water in three stages, one polybutadiene-coated mild steel, second nanocoated octahydrobenzo [a,d][8]annulene5,12-dihydrazone and third was coated with MgS. The corrosion rate of each material was calculated by weight loss formula  $K(\text{mmpy}) = \frac{3.56 W}{D A t}$  (where W = weight loss of test coupon expressed in kg, A = area of test coupon in square meter, D = Density of the material in kg. m<sup>-1</sup>) at 283, 293, 303, 312 and 3230K temperatures and time

mentioned 3, 5, 8, 11 and 14 days. Their corrosion rate recorded in Table 1 and the results of Table 1 indicated that in marine water corrosion rate of polybutadiene e-coated mild steel increased but its values decreased with the nanocoating of nanocoated and filler compounds. The plot between  $K(\text{mmpy})$  versus  $t(\text{days})$  in Figure 15 confirmed the above mentioned trends. The corrosion rate of polybutadiene increased with nanocoated octahydrobenzo[a,d][8]dihydrazone but this decreased with MgS filler, it observed different interval of times. Polybutadiene-coated mild steel face severe crevice corrosion problem due to depletion of  $\text{O}_2$  inside and outside of polybutadiene. The use of nanocoating of octahydrobenzo[a,d][8]dihydrazone and MgS filler create composite thin film barrier which is more stable in

marine water. This barrier is thermally stable and suppresses the attack of corrosive ions. MgS is active compounds which are entered into porosities of octahydrobenzo[a,d][8]annulene-5,12-dihydrazone and forms complex this nitrogen containing compound. This surface film attaches with base materials by chemical bonding and forms a passive layer. There was studied the effect of temperatures at 283, 293, 303, 313 and 323 K on polybutadiene-coated mild steel and after nanocoated with octahydrodibenzo[a,d][8]annulene-5,12-dihydrazone and MgS filler, it was observed that with the rise of temperatures corrosion enhanced but nanocoating and filler compounds reduced their values. This effect clearly depicted in Table 1 and Figure 16 which plotted between  $\log K$  versus  $1/T$ .

### ChemNMR $^1\text{H}$ Estimation



Estimation quality is indicated by color: **good**, **medium**, **rough**

Protocol of the  $^1\text{H}$ -NMR Prediction (Lib=SU Solvent=DMSO 300 MHz):

Node	Shift	Base + Inc.	Comment (ppm rel. to TMS)
CH 7.83	7.26	1-benzene	
	0.63	1-C (=O)CC	
	0.00	1-CC	
	-0.06	generalconnections	
CH 7.48	7.26	1-benzene	
	0.08	1-C (=O)CC	
	-0.08	1-CC	
	0.22	generalconnections	
CH 7.30	7.26	1-benzene	
	0.08	1-C (=O)CC	
	-0.10	1-CC	
	0.06	generalconnections	
CH 7.59	7.26	1-benzene	
	0.18	1-C (=O)CC	
	0.00	1-CC	
	0.15	generalconnections	
CH 3.16	1.44	cyclohexane	
	1.50	1 alpha-C (=O)-1 C *C *C *C *C *1 from methine	
	0.22	1 beta-C=O from methine	
CH 2.83	1.44	cyclohexane	
	0.86	1 alpha-C=O from methine	
	0.53	1 beta-C (=O)-1 C *C *C *C *C *1 from methine	
CH2 1.64,1.385000	1.44	cyclohexane	
	0.15	1 beta-C (=O)-1 C *C *C *C *C *1 from methylene	
	-0.08	generalconnections	
CH2 1.73,1.475000	1.44	cyclohexane	
	0.24	1 beta-C (=O)-C from methylene	
	-0.08	generalconnections	
CH2 1.53,1.430000	1.44	cyclohexane	
	0.04	generalconnections	
CH2 1.53,1.430000	1.44	cyclohexane	
	0.04	generalconnections	
CH2 2.83	1.37	methylene	
	1.22	1 alpha-1 C *C *C *C *C *1	
	0.24	1 beta-C (=O)-C	
CH2 2.83,2.730000	1.37	methylene	
	1.12	1 alpha-C (=O)-C	
	0.29	1 beta-1 C *C *C *C *C *1	

### $^1\text{H}$ NMR Coupling Constant Prediction

shift: atom index coupling partner, constant and vector

7.83	3	5	7.5	H-C *C-H
		6	1.5	H-C *CH *C-H
7.48	4	6	7.5	H-C *C-H
		5	1.5	H-C *CH *C-H
7.30	5	3	7.5	H-C *C-H
		6	7.5	H-C *C-H
		4	1.5	H-C *CH *C-H
7.59	6	4	7.5	H-C *C-H
		5	7.5	H-C *C-H
		3	1.5	H-C *CH *C-H
3.16	11	10	7.0	H-C *C-H
		16	7.0	H-C *CH *H
2.83	10	11	7.0	H-C *C-H
		13	7.0	H-C *CH *H
1.51	16	11	7.0	H-C *C-H
		15	7.1	H-C *CH *H
1.60	13	10	7.0	H-C *C-H
		14	7.1	H-C *CH *H
1.48	15	16	7.1	H-C *C-H
		14	7.1	H-C *CH *H
1.48	14	13	7.1	H-C *C-H
		15	7.1	H-C *CH *H
2.83	7	8	7.1	H-C *C-H
2.78	8	7	7.1	H-C *C-H

Figure 11.

The values of  $\log(\theta/1-\theta)$  for octahydrodibenzo[a,d][8]annulene-5,12-dihydrazone and MgS filler mentioned in Table 1 at different temperatures, it was found that  $\log(\theta/1-\theta)$  decreased with nanocoating material as increasing temperatures but its

values increased with filler as shown in Table 1 and Figure 17 which plotted between  $\log(\theta/1-\theta)$  versus  $1/T$ . The nanocoating and filler compounds developed a non osmosis barrier that neutralized the attack of  $\text{Cl}^-$  ions and  $\text{H}_2\text{CO}_3$ . The surface coverage



areas were covered by octahydrodibenzo[a,d][8]annulene-5,12-dihydrazone and MgS filler at various temperatures and calculated by formula  $\theta = (1 - K / K_o)$  (where K is the corrosion rate before coating and  $K_o$  is the corrosion rate after coating) and their values were written in Table 1. It was observed that nanocoating compound increased surface coverage area but filler improved the mitigation character of surface coverage area. Such types of trends noticed in Figure 18 which plotted between  $\theta$ (surface coverage area) versus T(temperature). The percentage coating efficiency of octahydrodibenzo[a,d][8]annulene-5,12-

dihydrazone and MgS filler were calculated by formula,  $\%CE = (1 - K / K_o) \times 100$  (where CE = coating efficiency, K = Corrosion rate with coating,  $K_o$  = corrosion rate without coating) and its values were mentioned in Table 1. These results show that nanocoating and filler compounds increased coating efficiency but filler enhanced more efficiency. Figure 19 plotted between  $\%CE$  (percentage coating efficiency) versus T (temperature), it was observed that MgS filler increased coating efficiency of nanocoating compound in marine water.

**Table 1:** Corrosion rate of polybutadiene-coated mild steel nanocoated with octahydrodibenzo [a,d] [8] annulene-5,12-dihydrazone [NC(1)]and MgS filler in  $SO_2$  environment

N C & F	Temp(OK)	2830K	2930K	3030K	3130K	3230K	C(mM )
	Time(days)	2	5	8	11	14	
NC(0) NC(1) F(MgS)	K	94.641	115.187	143.308	160.366	172.684	00 50 10
	logK	1.976	2.061	2.156	2.205	2.237	
	K	21.842	26.086	36.49	42.546	47.049	
	logK	1.339	1.416	1.562	1.628	1.672	
	log(K/T)	0.791	0.883	1.043	1.125	1.182	
	$\theta$	0.7692	0.7735	0.7453	0.7338	0.7225	
	(1- $\theta$ )	0.2308	0.2265	0.2562	0.2662	0.2725	
	( $\theta/1-\theta$ )	3.332	3.415	2.909	2.756	2.651	
	log( $\theta/1-\theta$ )	0.522	0.533	0.463	0.440	0.423	
	$\%CE$	76.92	77.35	74.53	73.38	72.75	
	K	17.671	19.847	24.385	26.471	28.129	
	logK	1.247	1.297	1.387	1.422	1.449	
	log(K/T)	0.699	0.764	0.868	0.918	0.959	
	$\theta$	0.8132	0.8276	0.8298	0.8349	0.8371	
	(1- $\theta$ )	0.1863	0.1724	0.1702	0.1651	0.1629	
	( $\theta/1-\theta$ )	4.353	4.801	4.862	5.056	5.138	
	log( $\theta/1-\theta$ )	0.638	0.681	0.686	0.703	0.711	
	$\%CE$	81.32	82.76	82.98	83.49	83.71	

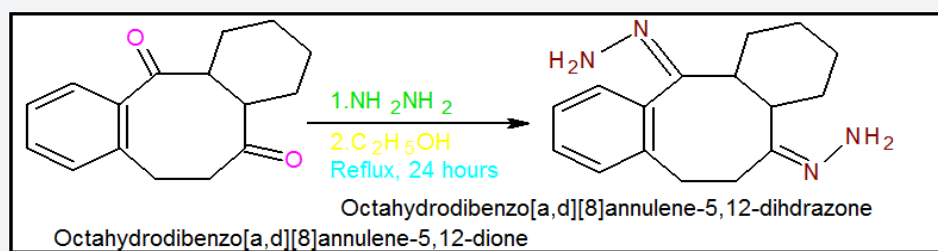


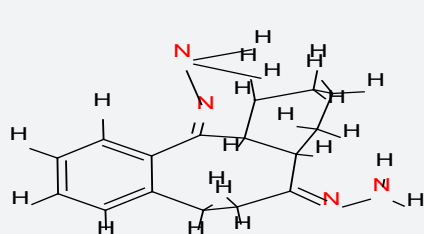
**Figure 12.**

Activation energy of polybutadiene-coated mild steel, octahydrodibenzo[a,d][8]annulene-5,12-dihydrazone and MgS filler were calculated by Figure 18. 8.2 and Arrhenius equation,  $d / dt (\log K) = E_a / R T^2$  (where T is temperature in Kelvin, R is universal gas constant and  $E_a$  is the activation energy of the reaction). The values of activation energies were expressed in Table 2 and plot between  $\log K$  versus  $1/T$  found to be straight lines

in figure 16. The positive values of activation energy indicated that nanocoated and filler compounds developed a thin film by chemical bonding. At higher temperature, activation energy reduced so both compounds formed stable barrier on the surface of base material. Heat of adsorption of octahydrodibenzo[a,d][8]annulene-5,12-dihydrazone and MgS filler were obtained by Langmuir equation,  $\log (\theta / 1-\theta) = \log (A . C) - (q / 2.303 R T)$

( where T is temperature in Kelvin and q heat of adsorption) and Figure 18. 8.3 a linear graph between  $\log(\theta / 1-\theta)$  verse  $1/T$ . Their values mentioned in Table 2 confirmed that nanocoating and filler compounds attached with base material by chemical bonding. Free energy of octahydrodibenzo[a,d][8]annulene-5,12-dihydrazone and MgS filler were determined by formula,

$\Delta G = -2.303RT \log(33.3K)$  (where R is universal gas constant, T be temperature and K corrosion rate) and their recorded values in Table 2 gave information during coating exothermic reaction occurred. The results of Table 2 noticed that nanocoating and filler compounds were adhered with base material by chemical bonding.



Molecular Formula	= C <sub>16</sub> H <sub>22</sub> N <sub>4</sub>
Formula Weight	= 270.37268
Composition	= C(71.08%) H(8.20%) N(20.72%)
Molar Refractivity	= 78.57 ± 0.5 cm <sup>3</sup>
Molar Volume	= 207.6 ± 7.0 cm <sup>3</sup>
Parachor	= 561.5 ± 8.0 cm <sup>3</sup>
Index of Refraction	= 1.681 ± 0.05
Surface Tension	= 53.5 ± 7.0 dyne/cm
Density	= 1.30 ± 0.1 g/cm <sup>3</sup>
Dielectric Constant	= Not available
Polarizability	= 31.14 ± 0.5 10 <sup>-24</sup> cm <sup>3</sup>
Monoisotopic Mass	= 270.184447 Da
Nominal Mass	= 270 Da
Average Mass	= 270.3727 Da
M+	= 270.183898 Da
M-	= 270.184995 Da
[M+H] <sup>+</sup>	= 271.191723 Da
[M+H] <sup>-</sup>	= 271.19282 Da
[M-H] <sup>+</sup>	= 269.176073 Da
[M-H] <sup>-</sup>	= 269.17717 Da

Figure 13.

**Table 2:** Thermal parameter of octahydrodibenzo [a,d] [8] annulene-5,12-dihydrazone and MgS filler nanocoating on polybutadiene-coated mild steel in marine water.

Thermal Parameters	2830K	2930K	3030K	3130K	3230K
Ea(0)	133.43	134.44	136.10	139.19	132.23
Ea, NC(1)	90.42	90.32	98.61	99.34	98.83
q „NC(1)	-35.25	-34.76	-29.23	-26.85	-25.01
ΔG,NC(1)	-193.24	-191.71	-194.72	-192.30	-188.86
ΔH, NC(1)	-53.45	-57.64	-65.88	-68.65	-69.90
ΔS, NC(1)	-69.88	-73.12	-78.96	-81.80	-83.74
θ, NC(1)	0.7692	0.7735	0.7453	0.7338	0.7275
Ea, F(MgS)	84.21	84.61	87.55	86.77	85.65
q „F(MgS)	-43.08	-44.42	-43.31	-42.90	-42.02
ΔG, F(MgS)	-187.03	-183.96	-183.67	-179.73	-175.65
ΔH, F(MgS)	-47.23	-49.89	-54.83	-56.08	-56.69
ΔS, F(MgS)	-66.36	-68.57	-72.27	-73.92	-75.19
θ, F(MgS)	0.8132	0.8276	0.8298	0.8349	0.8371

Enthalpy and entropy of octahydrodibenzo[a,d][8]annulene-5,12-dihydrazone and MgS filler were calculated by transition state equation,  $K = R T / N h \log(\Delta S \# / R) \times \log(-\Delta H \# / R T)$  (where N is Avogadro's constant, h is Planck's constant,  $\Delta S \#$  is the change of entropy activation and  $\Delta H \#$  is the change of enthalpy activation) and Figure 20 a linear graph between  $\log(K)$  versus  $1/T$  and their values were written in Table 2. Nanocoating and filler compounds exhibited negative values of enthalpy and entropy. This sign indicated that coating is an exothermic process. Nanocoating and filler compounds were accommodated on the surface of base material by chemical bonding. Entropy values determined that filler compound arranged into matrix

of nanocoating compound in ordered manner. Enthalpy and entropy of nanocoating of octahydrodibenzo[a,d][8]annulene-5,12-dihydrazone and ZnS filler indicate that the coating of both compounds is exothermic process. The results of all thermal parameters like activation energy, heat of adsorption, free energy, enthalpy and entropy at different temperatures were written in Table 2 and their graph plotted in Figure 21. After analysis of the results of all thermal parameters, it was found that surface coverage area increased as temperatures enhanced. The nanocoating and filler compounds formed thin surface film barrier on polybutadiene by chemical bonding that barrier stopped osmosis or diffusion process of marine water.



Potentiostat polarization results of polybutadiene-coated mild steel, octahydrodibenzo[a,d][8]annulene-5,12-dihydrazine and MgS filler were calculated by formula,  $\Delta E/\Delta I = \beta_a \beta_c / 2.303 I_{corr} (\beta_a + \beta_c)$  (where  $\Delta E/\Delta I$  is the slope which linear polarization resistance ( $R_p$ ),  $\beta_a$  and  $\beta_c$  are anodic and cathodic Tafel slope respectively and  $I$  is the corrosion current density in  $\text{mA}/\text{cm}^2$ ) and Tafel plot between  $\Delta E(\text{mV}$ , electrode potential) versus  $I(\text{mA}/\text{cm}^2$ , corrosion current density) in Figure 22 and their values were recorded in Table 3. It was observed that electrode potential and anodic current density was high with polybutadiene-coated

mild steel but these values decreased with nanocoating and filler compounds. Both compounds enhanced cathodic current density and reduced electrode potential. Corrosion current of polybutadiene-coated mild, octahydrodibenzo [a,d][8]annulene-5,12-dihydrazine and MgS filler were obtained by above equation and their values were put in equation,  $C. R (\text{mmpy}) = 0.1288 I_{corr} (\text{mA}/\text{cm}^2) \times \text{Eq. Wt} (\text{g}) / \rho (\text{g}/\text{cm}^3)$  (where  $I_{corr}$  is the corrosion current density  $\rho$  is specimen density and Eq.Wt is specimen equivalent weight) produced corrosion rate.

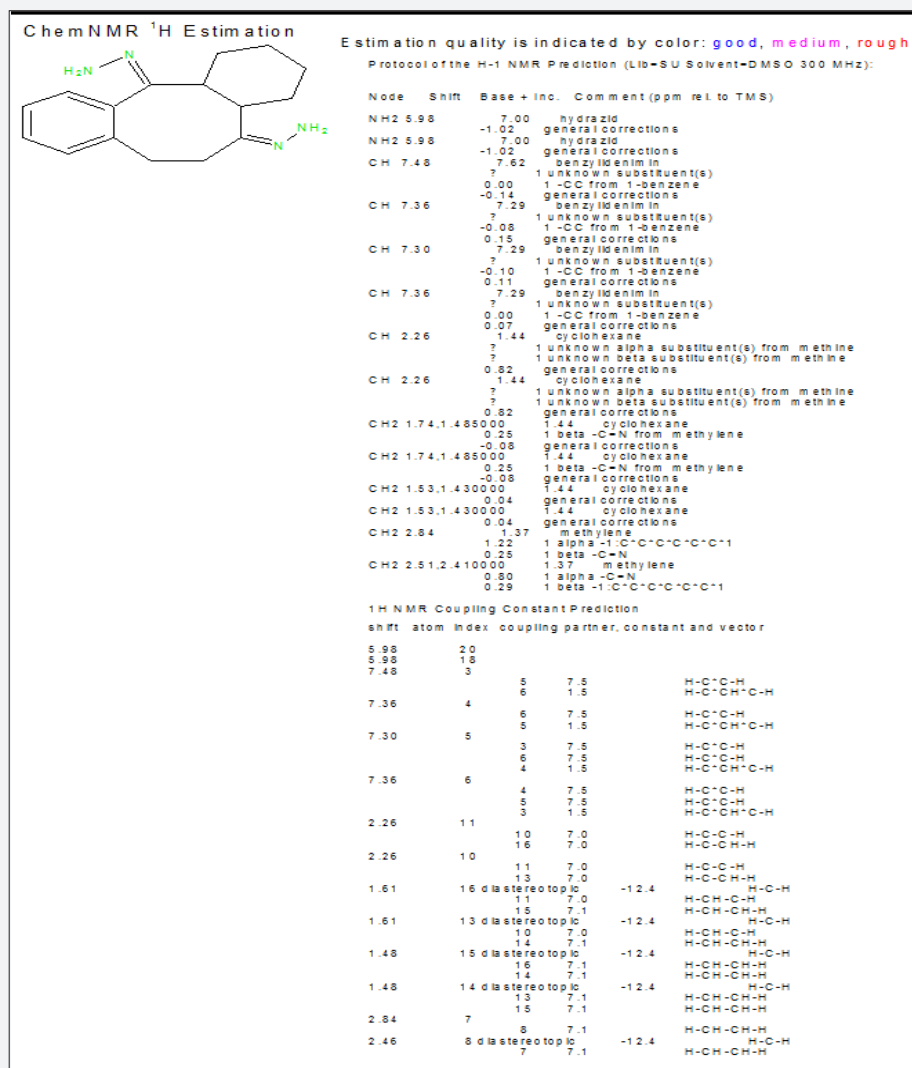


Figure 14.

The corrosion rate of all three materials were given in Table 3, it was observed that corrosion rate of polybutadiene-coated mild steel were high but these values were decreased with nanocoating and filler compounds. MgS filler enhanced cathodic current density and percentage coating efficiency with respect of octahydrodibenzo[a,d][8]annulene-5,12-dihydrazine. Filler compound reduced more corrosion rate with octahydrodibenzo[a,d][8]annulene-5,12-dihydrazine.

Nanocoating and filler form a composite thin film on the surface of polybutadiene-coated mild steel during coating and its stability is good in hostile marine water. The results were obtained by weight loss experiment for polybutadiene-coated mild steel in marine water by nanocoating of octahydrodibenzo[a,d][8]annulene-5,12-dihydrazine and MgS were tally with the results of potentiostat.

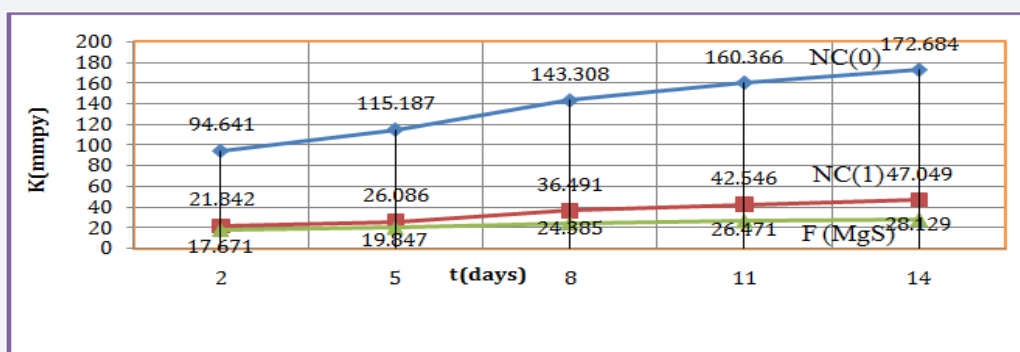


Figure 15. K(mmpy) Vs t(days) for nanocoating of NC(1) & MgS filler on polybutadiene-coated mild steel.

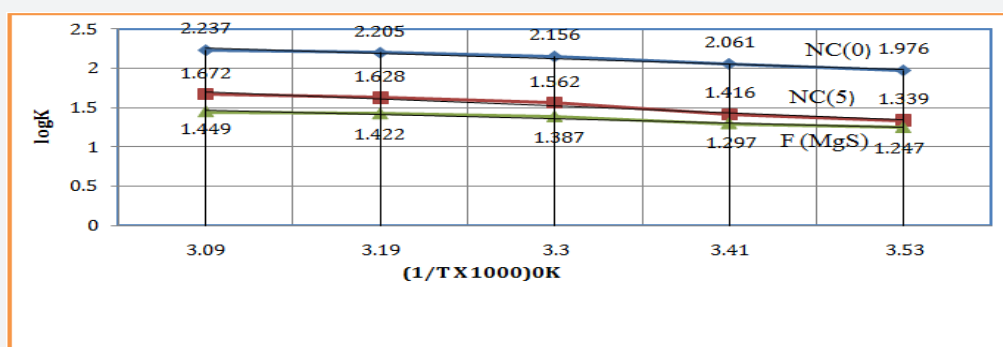


Figure 16. log K Vs 1/T for nanocoating of NC(6) & MgS filler on polybutadiene-coated mild steel.

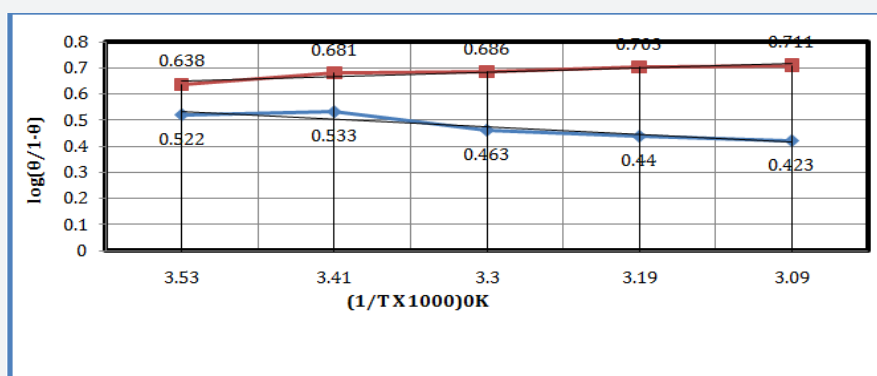


Figure 17. log (θ/1-θ) Vs 1/T for nanocoating of NC (1) & MgS filler on polybutadiene-coated mild steel.

Table 3: Potentiostatic polarization of nanocoating octahydrodibenzo[a,d] [8]annulene-5,12-dihydrazone and MgS filler on polybutadiene-coated mild steel.

NC	ΔE (mV)	ΔI	β <sub>a</sub>	β <sub>c</sub>	I <sub>corr</sub> (mA/cm <sup>2</sup> )	K (mmpy)	θ	% CE	C (mM)
NC(0)	-451	112	172	151	8.69	264.69	0	0	
NC(1)	-311	65	75	180	4.81	146.51	0.71	71	0.0
F(MgS)	-251	55	65	195	4.65	141.63	0.88	88	

## Conclusion

Octahydrodibenzo[a,d][8]annulene-5,12-dihydrazone and MgS filler used for the corrosion protection of polybutadiene-coated mild steel. These materials formed coating composite coating barrier on the surface of base polybutadiene-coated mild

steel. Nanocoating compounds and filler compounds thermal parameters were indicated that composite surface barrier creation was exothermic process. The corrosive environment did not produce corrosion cell. The coating efficiencies and surface coverage area of nanocoating and filler compounds enhanced in different temperatures, atmosphere and weather changes.

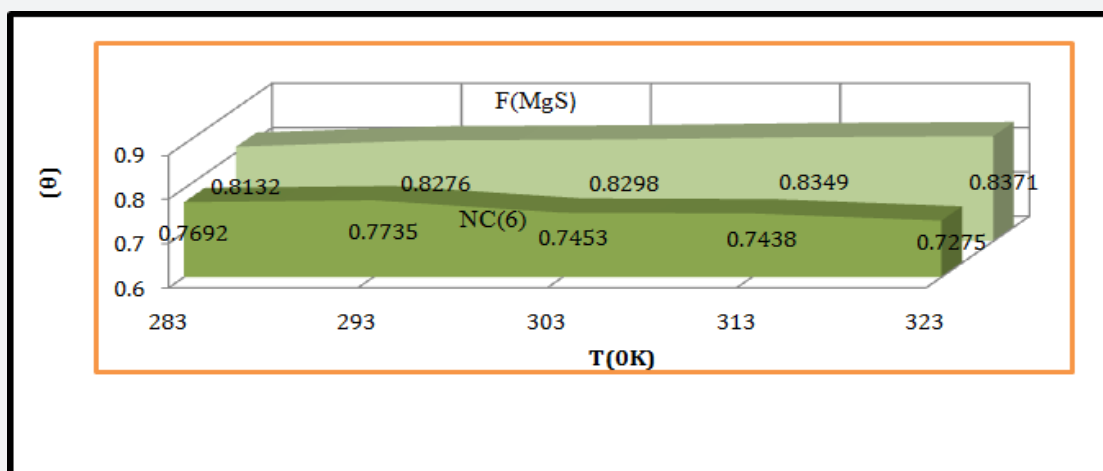


Figure 18.  $\theta$  Vs T for nanocoating of NC(1) & MgS filler on polybutadiene-coated mild steel.

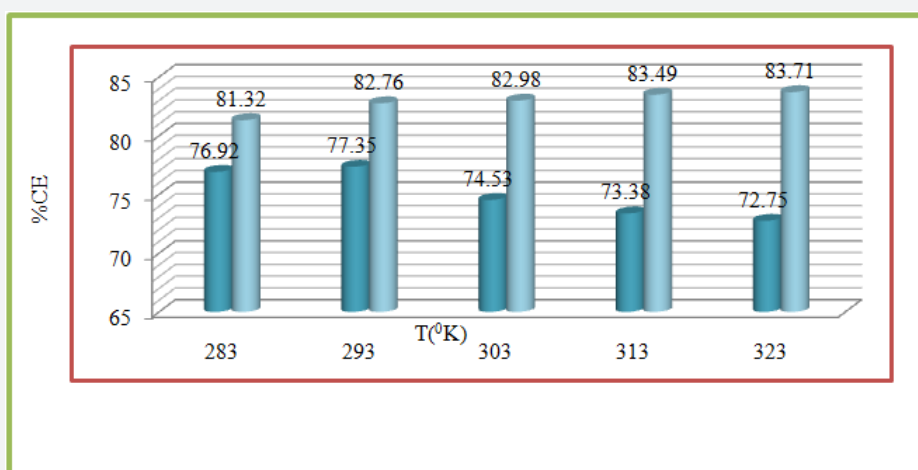


Figure 19. %CE Vs T for nanocoating of NC(1) & NC(F) on polybutadiene-coated mild steel.

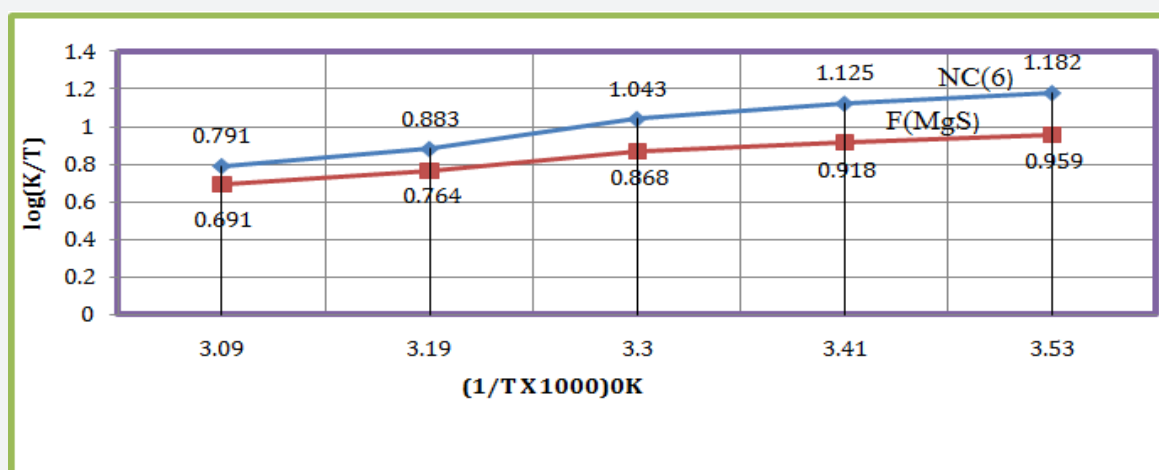


Figure 20.  $\log(K/T)$  Vs  $1/T$  for nanocoating of NC(6) & MgS filler on polybutadiene-coated mild steel.

## Acknowledgement

Authors thankful for UGC-New Delhi provided financial

support for this work. I give my thanks to laboratory staffs for their supports during experimental work.

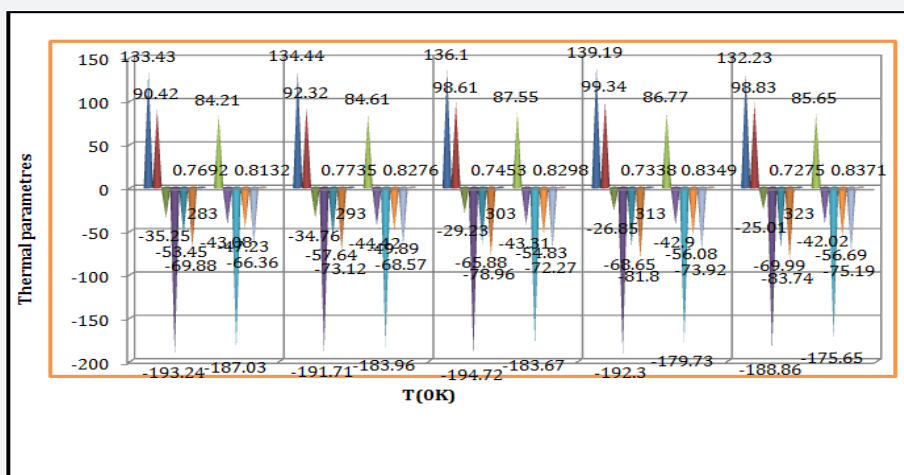


Figure 21. Thermal parameters Vs T for nanocoating of NC(1) & MgS on polybutadiene-coated on mild steel.

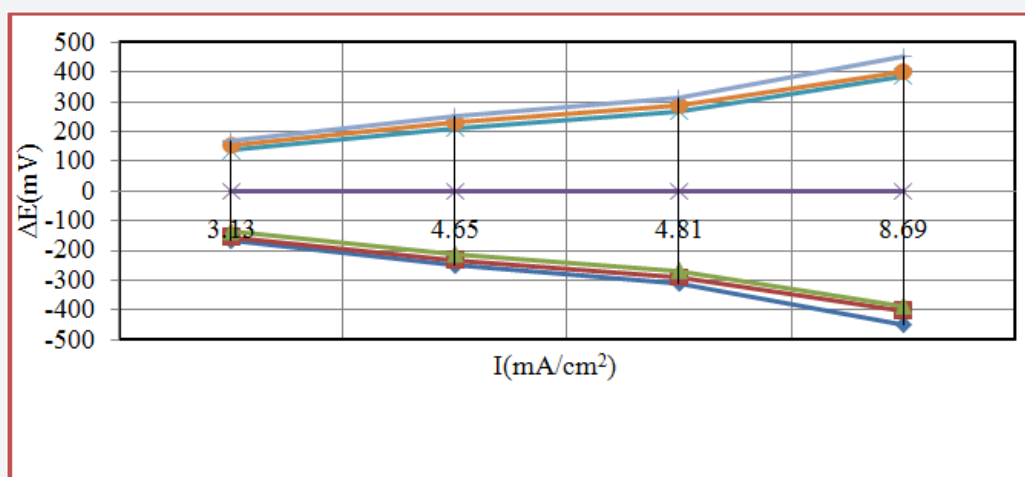


Figure 22.  $\Delta E$  (mV) Vs  $I$  (mA/cm<sup>2</sup>) for nanocoating of NC(1) & MgS filler on polybutadiene-coated mild steel.

## References

- Bhadra S, Singh NK, Khastgir D (2011) Polyaniline based anticorrosive and anti-molding coating. *Journal of Chemical Engineering and Materials Science* 2(1): 1-11.
- Szabo T, Molnar Nagy L, Telegdi J (2011) Self-healing microcapsules and slow release microspheres in paints. *Progress in Organic Coatings* 72(1-2): 52-57.
- Wen NT, Lin CS, Bai CY, Ger MD (2008) Structures and characteristics of Cr (III) based conversion coatings on electrogalvanized steels. *Surf Coat Technol* 203(3-4): 317-323.
- Boerio FJ, Shah P (2005) Adhesion of injection molded PVC to steel substrates. *J of Adhesion* 81(6): 645-675.
- Deveci H, Ahmetti G, Ersoz M (2012) Modified styrenes: Corrosion physico-mechanical and thermal properties evaluation. *Prog Org Coat* 73(1): 1-7.
- Genzer J (2005) Templating Surfaces with Gradient Assemblies. *J of Adhesion* 81(3-4): 417-435.
- Leon Silva U, Nicho ME (2010) Poly (3-octylthiophene) and polystyrene blends thermally treated as coating for corrosion protection of stainless steel 304. *J Solid State Electrochem* 14(8): 1487-1497.
- Baier RE (2006) Surface behaviour of biomaterials: Surface for biocompatibility. *J Mater Sci Mater Med* 17(11): 1057-1062.
- Rao BVA, Iqbal MY, Sreehar B (2010) Electrochemical and surface analytical studies of the self assembled monolayer of 5-methoxy-2-(octadecylthiol) benzimidazole in corrosion protection of copper. *Electrochim Acta* 55(3): 620-631.
- Liu XY, Ma HY, Hou MZ (2009) Self-assembled monolayers of stearic imidazoline on copper electrodes detected using electro chemical measurement, XPS, molecular simulation and FTIR. *Chinese Sci Bull* 54(3): 374-381.
- Liao QQ, Yue ZW, Zhou Q (2009) Corrosion inhibition effect of self-assembled monolayers of ammonium pyrrolidine dithiocarbamate on copper. *Acta Phys Chin Sin* 25(8): 1655-1661.
- Zhang DQ, He XM, Kim GS (2009) Arginine self-assembled monolayers against copper corrosion and synergetic effect of iodide ion. *J Appl Electrochem* 39(8): 1193-1198.
- Sahoo RR, Biswas SK (2009) Frictional response of fatty acids on steel. *J Colloid Interf Sci* 333(2): 707-718.
- Raman R, Gawalt ES (2007) Selfassembled monolayers of alkanolic acid on the native oxide surface of SS316L by solution deposition. *Langmuir* 23(5): 2284-2288.

15. Li DG, Chen SH, Zhao SY (2006) The corrosion Inhibition of the self-assembled Au and Ag nanoparticles films on the surface of copper, Colloid. Surface A 273(1-3): 16-23.
16. Cristiani P, Perboni G, Debenedetti A (2008) Effect of chlorination on the corrosion of Cu|Ni 70|30 condenser tubing. Electrochim Acta 54(1): 100-107.
17. Cristiani P (2005) Solutions fouling in power station condensers. Appl Therm Eng 25(16): 2630-2640.
18. Videla H, Herrera LK (2009) Understanding microbial inhibition of corrosion. Electrochem Acta 39:229-234.
19. Bibber JW (2009) Chromium free conversion coating for zinc and its alloys. Journal of Applied Surface Finishing 2(4): 273-275.
20. Ghareba GS, Omanovic S (2010) Interaction of 12-aminododecanoic acid with a carbon steel surface: Towards the development of 'green' corrosion inhibitors. Corrosion Sci 52(6): 2104-2113.
21. Singh RK (2016) Corrosion protection of transport vehicles by nanocoating of decahydrobenzo[8]annulene-5,10-dihydrazone and SiC filler in H<sub>2</sub>O(moist), CO<sub>2</sub>, SO<sub>2</sub> environments and weather change. Journal of Metallurgy and Materials Science 58: 167-179.
22. Singh RK (2017) Corrosion protection of transport vehicles by nanocoating of decahydrobenzo[8]annulene-5,10-dihydrazone in corrosive environments and weather change. Journal of Powder Metallurgy & Mining 1: 2-8.
23. Singh R K (2017) Atmospheric corrosion protection of epoxy-coated stainless steel by nanocoating of decahydrobenzo[8]annulene-5,10-disemecarbazone and TiN filler. International J of NME 2(4): 17-32.



This work is licensed under Creative Commons Attribution 4.0 License  
DOI: [10.19080/JOJMS.2018.07.555637](https://doi.org/10.19080/JOJMS.2018.07.555637)

## Your next submission with Juniper Publishers will reach you the below assets

- Quality Editorial service
- Swift Peer Review
- Reprints availability
- E-prints Service
- Manuscript Podcast for convenient understanding
- Global attainment for your research
- Manuscript accessibility in different formats  
( Pdf, E-pub, Full Text, Audio)
- Unceasing customer service

Track the below URL for one-step submission  
<https://juniperpublishers.com/online-submission.php>